Spin-Orbit Coupled Weakly Interacting Bose-Einstein Condensates in Harmonic Traps

Hui Hu, B. Ramachandhran, Han Pu, and Xia-Ji Liu

Phys. Rev. Lett. **108**, 010402 — Published 4 January 2012

DOI: 10.1103/PhysRevLett.108.010402

Spin-orbit coupled weakly interacting Bose-Einstein condensates in harmonic traps

Hui Hu[1], B. Ramachandhran[2], Han Pu[2], and Xia-Ji Liu[1]
[1] *ACQAO and Centre for Atom Optics and Ultrafast Spectroscopy, Swinburne University of Technology, Melbourne 3122, Australia*
[2] *Department of Physics and Astronomy, and Rice Quantum Institute, Rice University, Houston, TX 77251, USA*
(Dated: November 17, 2011)

We investigate theoretically the phase diagram of a spin-orbit coupled Bose gas in two-dimensional harmonic traps. We show that at strong spin-orbit coupling the single-particle spectrum decomposes into different manifolds separated by $\hbar\omega_\perp$, where $\omega_\perp$ is the trapping frequency. For a weakly interacting gas, quantum states with skyrmion lattice patterns emerge spontaneously and preserve either parity symmetry or combined parity-time-reversal symmetry. These phases can be readily observed in a spin-orbit coupled gas of ^{87}Rb atoms in a highly oblate trap.

PACS numbers: 05.30.Jp, 03.75.Mn, 67.85.Fg, 67.85.Jk

Spin-orbit (SO) coupling leads to many fundamental phenomena in a wide range of quantum systems from nuclear physics, condensed matter physics to atomic physics. For instance, in electronic condensed matter systems SO coupling can lead to quantum spin Hall states or topological insulators [1], which have potential applications in quantum devices. Recently, SO coupling has been induced in ultracold spinor Bose gases of ^{87}Rb atoms [2] by the so-called "synthetic non-Abelian gauge fields". Combined with unprecedented controllability of interactions and geometry in ultracold atoms, this manipulation of SO coupling opens an entirely new paradigm for studying strong correlations of quantum many-body systems under non-Abelian gauge fields.

In this context, over the past few years there have been great theoretical efforts to determine quantum states of an SO coupled spinor Bose-Einstein condensate (BEC) [3–9]. In a recent work by Wang *et al.* [6], two distinct phases are identified for a *homogeneous* two-dimensional (2D) spin-1/2 BEC. Depending on the relative magnitude of intra-species (g) and inter-species ($g_{\uparrow\downarrow}$) interactions, all bosons can condense into either a single plane-wave state ($g < g_{\uparrow\downarrow}$) or a density-stripe state ($g > g_{\uparrow\downarrow}$).

The purpose of this Letter is to show that the presence of a *harmonic trap*, which is necessary in experiments, can change dramatically the phase diagram of SO coupled BECs. At strong SO coupling the single-particle spectrum decomposes into discrete manifolds, analogous to discrete Landau levels. Non-trivial quantum states with skyrmion lattices emerge when all bosons occupy into the lowest manifold (LM). These properties are fundamentally different from that of a homogeneous system. We note that, in a previous work, the NIST group has experimentally realized an artificial Abelian gauge field which leads to the observation of vortex lattice in a non-rotating ^{87}Rb condensate [10]. Our work represents an important extention into the regime of non-Abelian gauge field in which the spin degrees of freedom play an essential role.

Our main results are summarized in Fig. 1, which shows the ground state as functions of interatomic interaction at a dimensionless SO coupling strength $\tilde{\lambda}$. By using mean-field theory and exact diagonalization, we find that: (**i**) The ground state falls into two classes of quantum phases, I and II, preserving respectively the parity ($\mathcal{P}$) and parity-time-reversal ($\mathcal{PT}$) symmetries. Both symmetries are satisfied by the model Hamiltonian [see Eqs. (1) below]. (**ii**) In each class, there are several subphases (IA, IA′, IB and IIA, IIB) differing in the density distribution and/or total angular momentum. (**iii**) The transition between different phases depends on inter-

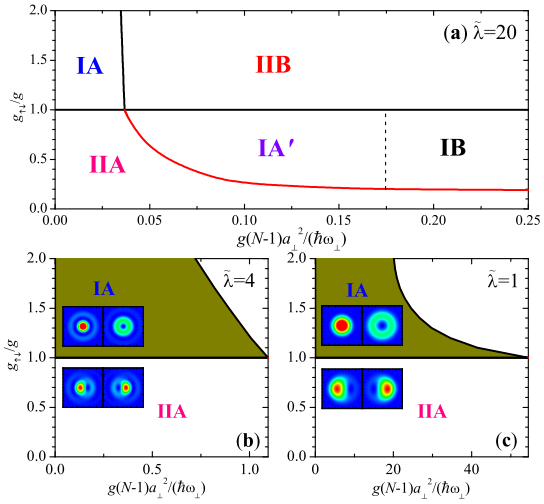

Figure 1: (color online). (**a**) Phase diagram of a trapped 2D BEC with a strong SO coupling $\tilde{\lambda} = 20$, where the single-particle spectrum forms discrete manifolds. For the weak interaction considered here, only the LM is occupied. The phases I and II preserve, respectively, the parity and parity-time-reversal symmetries. There are several sub-phases indicated by A, A′ and B, which differ in the density profile and/or angular momentum. The mean-field density patterns in different phases of spin-up bosons are shown in Fig. 3. (**b**) and (**c**) Phase diagram at weak SO coupling. Here the phases are determined without the restriction to the LM approximation. The insets illustrate the density profiles of the two spin components in phases IA and IIA.

atomic interactions. At weak intra-species interactions below a critical value, $g < g_c$, the ground state is a half-quantum vortex state (IA) if $g < g_{\uparrow\downarrow}$ and a superposition of two degenerate half-quantum vortex states (IIA) otherwise. The phases IA and IIA vanish in the limit of strong SO coupling, but dominate the phase diagram in the opposite. When the intra-species interactions becomes larger ($g > g_c$), there is an interesting reverse of the symmetry class, i.e., interactions change the phase IA into IIB and the phase IIA into IA$'$ and then IB. In the phases IIB and IB, skyrmion lattices emerge spontaneously without rotation. (**iv**) At $g = g_{\uparrow\downarrow}$, the phases are ordered by quantum fluctuations. Using exact diagonalization, we find that the phases follow those at $g < g_{\uparrow\downarrow}$.

Model Hamiltonian and energy spectrum. - We consider N-bosons in a 2D harmonic trap $V(\rho) = M\omega_\perp^2\rho^2/2$ with a Rashba SO coupling $\mathcal{V}_{so} = -i\lambda_R(\partial_y\hat{\sigma}_x - \partial_x\hat{\sigma}_y)$, where $\hat{\sigma}_{x,y,z}$ are the Pauli matrices. The model Hamiltonian is given by $\mathcal{H} = \mathcal{H}_0 + \mathcal{H}_{int}$, where

$$\mathcal{H}_0 = \int d\mathbf{r}\Psi^+\left[-\hbar^2\nabla^2/(2M) + V(\rho) + \mathcal{V}_{so}\right]\Psi, \quad (1a)$$

$$\mathcal{H}_{\rm int} = \int d\mathbf{r}\left[(g+g_{\uparrow\downarrow})\hat{n}^2 + (g-g_{\uparrow\downarrow})\hat{S}_z^2\right]/4\,, \quad (1b)$$

$\Psi = [\Psi_\uparrow(\mathbf{r}), \Psi_\downarrow(\mathbf{r})]^T$ denotes collectively the spinor Bose field operators, and $\hat{n}, \hat{S}_z = \Psi_\uparrow^+\Psi_\uparrow \pm \Psi_\downarrow^+\Psi_\downarrow$. We define two characteristic lengths, $a_\perp = \sqrt{\hbar/(M\omega_\perp)}$ for the harmonic trap and $a_\lambda = \hbar^2/(M\lambda_R)$ for the SO coupling. The dimensionless SO coupling strength can be then defined as $\tilde{\lambda} = a_\perp/a_\lambda = (M/\hbar^3)^{1/2}\lambda_R/\omega_\perp^{1/2}$. The Hamiltonian is invariant under two symmetry operations, associated respectively with the anti-unitary time-reversal operator $\mathcal{T} = i\sigma_y\mathcal{C}$, where $\mathcal{C}$ takes the complex conjugate, and the unitary parity operator $\mathcal{P} = \sigma_z\mathcal{I}$, where $\mathcal{I}$ is the spatial inversion operator. The Hamiltonian is also invariant under the combined $\mathcal{PT}$ operator, which is unitary since $\mathcal{P}$ and $\mathcal{T}$ anti-commute with each other, i.e., $\{\mathcal{P}, \mathcal{T}\} = 0$.

In polar coordinates (ρ, φ), the single-particle eigenwavefunctions of $\mathcal{H}_0$ may be written in the form, $\Phi_m(\mathbf{r}) = [\phi_\uparrow(\rho)e^{im\varphi}, \phi_\downarrow(\rho)e^{i(m+1)\varphi}]^T$, which is energetically degenerate with its time reversed partner $\mathcal{T}\Phi_m(\mathbf{r}) = [\phi_\downarrow(\rho)e^{-i(m+1)\varphi}, -\phi_\uparrow(\rho)e^{-im\varphi}]^T$. This degeneracy is a direct consequence of the Kramers' Theorem. Here we may restrict m to be non-negative integers, as a negative m state can be regarded as the time reversal partner for a state with $m \geq 0$. In this construction, Φ_m and $\mathcal{T}\Phi_m$ are both parity eigenstates with corresponding eigenvalues $(-1)^m$ and $(-1)^{m+1}$, respectively. However, they break the $\mathcal{PT}$ symmetry. The lowest single-particle state occurs at $m = 0$ and has a half-quantum vortex configuration [4]. Due to the degeneracy, any linear superposition of Φ_m and $\mathcal{T}\Phi_m$ — which breaks the parity symmetry — is also an eigenstate of the system. In particular, we may choose the equal-weight superposition as $(\Phi_m + \mathcal{T}\Phi_m)/\sqrt{2}$ which can be easily shown to be eigenstates of $\mathcal{PT}$.

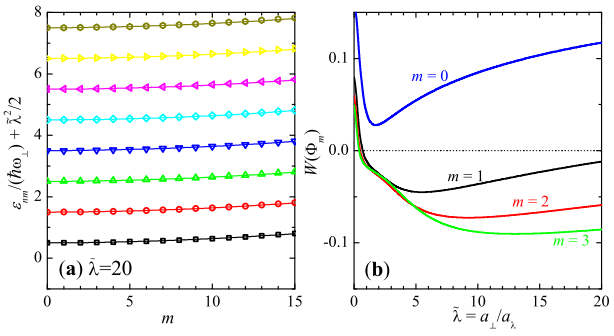

Figure 2: (color online). (a) Single-particle energy spectrum. The lines show the empirical Eq. (2). (b) The W-function for the lowest four single-particle states in the LM.

The wavefunctions and the corresponding eigenenergies can be found numerically. At large SO coupling (i.e., $\tilde{\lambda} > 5$), to a good approximation we find numerically that the low-lying spectrum forms discrete manifolds with spacing $\hbar\omega_\perp$ (indexed by an integer $n \geq 0$),

$$\epsilon_{nm} \simeq \left[-\tilde{\lambda}^2 + (2n+1) + m\,(m+1)/\tilde{\lambda}^2\right]\hbar\omega_\perp/2\,. \quad (2)$$

There are about $2\sqrt{2}\tilde{\lambda}$ levels within each manifold with the smallest level spacing $\Delta E = \hbar\omega_\perp/\tilde{\lambda}^2$. The discrete manifolds of spectrum are similar to the well-known Landau levels, formed when a charged particle moves in magnetic fields. However, the reasons for their formation are very different. In our case of large SO coupling, without trap the spectrum is characterized by a continuous momentum $\mathbf{k}$ and is given by $\epsilon_{\mathbf{k}} = [-\tilde{\lambda}^2/2 + (k \pm \tilde{\lambda})^2/2]\hbar\omega_\perp$, with infinite degeneracy along the azimuthal direction. The inclusion of trapping potential quantizes the radial motion for $\mathbf{k}$ and the azimuthal motion, giving the standard quantization contribution of $(n+1/2)\hbar\omega_\perp$ and $(m+1/2)^2/(2\tilde{\lambda}^2)\hbar\omega_\perp$ to the energy, respectively.

For a weakly interacting BEC with gN, $g_{\uparrow\downarrow}N \ll \hbar\omega_\perp$, only the LM is occupied. It is thus convenient to expand the field operator $\Psi = \sum_m \Phi_m(\mathbf{r})a_m$, where $\Phi_m(\mathbf{r})$ is the single-particle wavefunctions at the LM with energy ϵ_m. The many-body Hamiltonian may then be rewritten as,

$$\mathcal{H} = \sum_m \epsilon_m a_m^+ a_m + \sum_{ijkl} V_{ijkl} a_i^+ a_j^+ a_k a_l, \quad (3)$$

where the interaction elements V_{ijkl} can be calculated straightforwardly for the contact interatomic interactions. We solve Eq. (3) numerically by using both mean-field theory [11] and exact diagonalization [12], for a conserved total angular momentum $\sum_m (m+1/2)a_m^+ a_m = Nm_{tot}$. Within mean-field, we replace a_m by a complex number $N^{1/2}c_m$ and minimize the GP energy $E_{GP}/N = \sum_m \epsilon_m |c_m|^2 + (N-1)\sum_{ijkl} V_{ijkl}c_i^* c_j^* c_k c_l$, under the constraints $\sum_m |c_m|^2 = 1$ and $\sum_m (m+1/2)|c_m|^2 = m_{tot}$.

In practice, we truncate the angular momentum to $|m| \leq m_c$ (up to $m_c = 16$).

Symmetry of condensate states. - In the presence of the interaction represented by Eq. (1b), the many-body Hamiltonian still possesses both $\mathcal{P}$ and $\mathcal{PT}$ symmetries. As we have shown above, for a non-interacting system, we may choose the single-particle ground state to be an eigenstate of $\mathcal{P}$, or of $\mathcal{PT}$, or of neither operator. In the mean-field level, this freedom of choosing different symmetry eigenstates may be removed by inter-atomic interactions. In other words, the symmetry of condensate states would be determined *spontaneously* by interaction. We have found that in the weakly interacting limit we are interested in here, the ground state is either an eigenstate of $\mathcal{P}$, or that of $\mathcal{PT}$. Which symmetry the ground state will possess can be determined in the following way. Let us consider an eigenstate of $\mathcal{P}$ with wavefunction $\Phi_{\mathcal{P}} = [\phi_\uparrow(\mathbf{r}), \phi_\downarrow(\mathbf{r})]^T$. The corresponding eigenstate of $\mathcal{PT}$ can be constructed as $\Phi_{\mathcal{PT}} = (\Phi_{\mathcal{P}} \pm \mathcal{T}\Phi_{\mathcal{P}})/\sqrt{2}$. The mean-field energy difference between these two states is determined by the S_z^2 term in Eq. (1b) which breaks the spin rotational symmetry in the interaction Hamiltonian:

$$\Delta E_{sp}(\Phi) = E(\Phi_{\mathcal{PT}}) - E(\Phi_{\mathcal{P}}) = (g_{\uparrow\downarrow} - g) W(\Phi)/4, \quad (4)$$

where $W(\Phi) \equiv \int d\mathbf{r}[(|\phi_\uparrow|^2 - |\phi_\downarrow|^2)^2 - (\phi_\uparrow\phi_\downarrow + \phi_\uparrow^*\phi_\downarrow^*)^2]$. The ground state will be a $\mathcal{P}$-eigenstate if $\Delta E_{sp}(\Phi) > 0$ for which we have $n_\sigma(\mathbf{r}) = n_\sigma(-\mathbf{r})$, or a $\mathcal{PT}$-eigenstate if $\Delta E_{sp}(\Phi) < 0$ for which we have $n_\uparrow(\mathbf{r}) = n_\downarrow(-\mathbf{r})$. The W-functions of several parity eigenstates are shown in Fig. 2(b). Equation (4) also shows that the symmetry of the ground state is sensitive to the relative magnitude of the interaction parameters g and $g_{\uparrow\downarrow}$.

Phase diagram in the LM. - Our symmetry argument suggests that all the condensate states could be classified by its $\mathcal{P}$ or $\mathcal{PT}$ symmetry, to be referred to respectively as phases I and II hereafter. We now check numerically this argument in the quantum Hall like regime with all bosons occupying into the LM, as shown in Fig. 1(a) for $\tilde{\lambda} = 20$. The characteristic density distributions for spin-up bosons in each phase are shown in Fig. 3.

At sufficiently weak interactions, where the characteristic interaction energy $g(N-1)a_\perp^2$ is smaller than the lowest intra-manifold spacing $\Delta E = \hbar\omega_\perp/\tilde{\lambda}^2$, only the ground single-particle state is occupied. The condensate state is thus either half-quantum vortex states of Φ_0 (or $\mathcal{T}\Phi_0$) or their superposition. As $W(\Phi_0) > 0$ as shown in Fig. 2(b), we conclude that the ground state is a $\mathcal{PT}$-eigenstate for $g > g_{\uparrow\downarrow}$ (IIA) and it is a half-quantum vortex state (a $\mathcal{P}$-eigenstate) for $g < g_{\uparrow\downarrow}$ (IA). Their spin-up density patterns are shown in Figs. 3(a) and (d), respectively.

When the interaction becomes larger, more and more single-particle states are occupied. The occupation of the first excited single-particle state (Φ_1 and $\mathcal{T}\Phi_1$) occurs at $g_c(N-1)a_\perp^2 \simeq 0.0367\hbar\omega_\perp$, where the critical

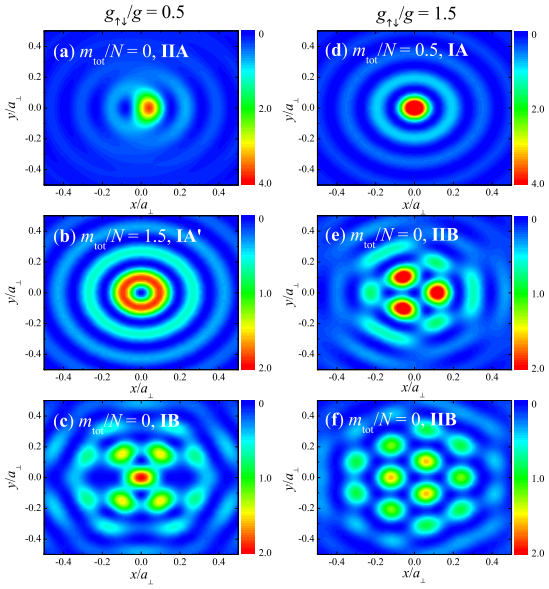

Figure 3: (color online). Density patterns of spin-up bosons in the different ground states at three intra-species interactions $g(N-1)a_\perp^2$: (a,d) $0.02\hbar\omega_\perp$, (b,e) $0.1\hbar\omega_\perp$, and (c,f) $0.2\hbar\omega_\perp$.

interaction strength g_c is determined from the equation $\epsilon_0 + (N-1)V_{0000} = \epsilon_1 + (N-1)V_{1111}$. As $W(\Phi_m) < 0$ for $m \geq 1$, we find an interesting reverse of the phase diagram when $g > g_c$: the $\mathcal{P}$-preserving phase (IA) changes into a $\mathcal{PT}$-preserving phase (IIB) at $g < g_{\uparrow\downarrow}$, while the $\mathcal{PT}$-preserving phase (IIA) changes into a $\mathcal{P}$-preserving phase (IA$'$ and IB) if $g > 0.2g_{\uparrow\downarrow}$. The phases IA$'$ and IB differ in the total angular momentum m_{tot} and density distribution. In Phase IB, m_{tot} is suppressed to zero by large interatomic interactions. Note that in the phases (IIB) and (IB), we observe regular lattice patterns. In particular, a hexagonal lattice form gradually in the phase IIB, as shown clearly in Figs. 3(e) and (f). In Fig. 4, we show the corresponding spin texture of the state, from which one can see that the system represents a lattice of skyrmions. Skyrmion lattice can be generated by rotating a spinor condensate [13]. Here the skyrmion texture is induced by the SO coupling without rotation.

The symmetry of the ground state at $g = g_{\uparrow\downarrow}$ can not be determined within mean-field theory, since in this case $\Delta E_{sp}(\Phi) = 0$ [see Eq. (4)] and the energy becomes invariant for different m_{tot}. However, it can be ordered by quantum fluctuations [4], which are well captured by exact diagonalization. We have calculated the energy as a function of m_{tot} at $g(N-1)a_\perp^2/(\hbar\omega_\perp) = 0.02$ and 0.1 for $N = 4$, 8, and 12. With increasing N, the exact diagonalization result approaches the mean-field prediction. We find that the ground state at $g(N-1)a_\perp^2 = 0.02\hbar\omega_\perp$ has a spontaneous angular momentum $m_{tot} = -1/2$ or $+1/2$, while the ground state at $g(N-1)a_\perp^2 = 0.1\hbar\omega_\perp$ occurs at $m_{tot} = 0$. Therefore, we identify that the phases at $g = g_{\uparrow\downarrow}$ follow those at $g < g_{\uparrow\downarrow}$. This is in agreement

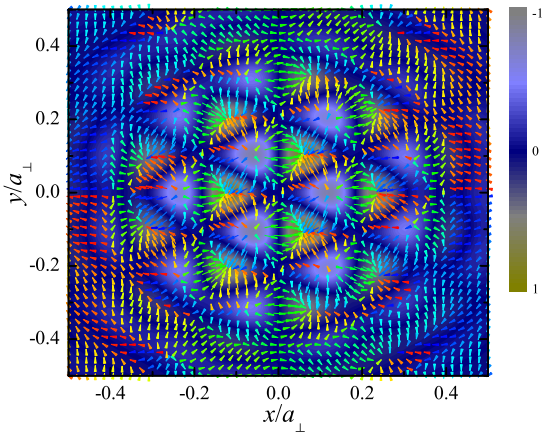

Figure 4: (color online). Spin texture $\mathbf{S} = (1/2)\Phi^+\sigma\Phi$ corresponding to the state represented in Fig. 3(f). The arrows represent the transverse spin vector (S_x, S_y) with color and length representing the orientation and the magnitude of the transverse spin. The contour plot shows the axial spin $S_z = (1/2)\left(\phi_\uparrow^2 - \phi_\downarrow^2\right)$.

with the result of Ref. [4], which employs a different "order from disorder" argument.

Phase diagram beyond LM. - So far we have clarified the phase diagram at a particular SO coupling $\tilde{\lambda} = 20$ in the *weakly-interacting* LM regime. However, the qualitative picture of diagram may persist beyond the regime of LM, as far as our symmetry argument holds. To check this, we performed a direct numerical calculation based on the full Gross-Pitaevskii (GP) equation derived from Eqs. (1) without making the LM assumption. In the regime as shown in Fig. 1(a), the results are in good agreement with the LM calculation. At larger interaction strength when higher manifolds get mixed in the ground state, we have found from the GP calculation that Phase IIB in Fig. 1(a) will change to a density-stripe phase with $\mathcal{P}$ symmetry, while Phase IB will change to a plane-wave phase with $\mathcal{PT}$ symmetry. The density-stripe and the plane-wave phases have been shown to be the mean-field ground state for a *homogeneous* system [6]. For the trapped system as studied here, at large interaction strength, the effect of the trap becomes less important and our results are therefore consistent with those reported in Ref. [6]. With decreasing $\tilde{\lambda}$, we anticipate that the phases IA and IIA will gradually become dominant in the diagram, as we find numerically that $g_c \propto 1/\tilde{\lambda}^2$ increases very rapidly. The skyrmion lattice phase, related to the LM formation, may disappear. This is confirmed by the GP calculation for smaller SO coupling and the results are represented in Fig. 1 (b) and (c). The half-quantum vortex state and its superposition dominate over a much larger parameter space as compared to the large SO coupling case. A more detailed study of the complete phase diagram and the properties of different phases will be presented elsewhere [14].

Experimental relevance. - We finally consider the experimental feasibility. A Rashba SO coupling can be induced in spinor ^{87}Rb gases [2]. The interaction strengths of ^{87}Rb atoms may be tuned by properly choosing the parameters of the laser fields that induce the SO coupling [8]. The two-dimensionality in such system has now been routinely realized by imposing a strong harmonic confinement $V(z) = M\omega_z^2 z^2/2$ along the z-direction with $\omega_z \gg \omega_\perp$. The critical temperature for an ideal 2D SO BEC is given by $T_c = (c_\lambda/\pi)\sqrt{3N}\hbar\omega_\perp/k_B$, where the prefactor $c_\lambda < 1$ takes into accout the suppression due to the SO coupling. Taking parameters from a recent experiment [15] with $\omega_\perp = 2\pi \times 20.6$ Hz and $N \sim 10^5$, we find at $\tilde{\lambda} = 10$, $c_\lambda \sim 0.6$ and $k_B T_c \simeq 120$ nK. Experimentally, BEC temperature below 0.5 nK has been recorded [16], which is also lower than $\hbar\omega_\perp/k_B$. The mean-field LLL regime is therefore readily attainable with current technologies.

Conclusion. - In summary, we have investigated the phase diagram of a spin-orbit coupled spinor BEC in harmonic traps, by using mean-field theory and exact diagonalization method. We have predicted that the condensate states preserve the parity or parity-time-reversal symmetry and exhibit spontaneous vortex and skyrmion lattice structure in the lowest energy manifold which is induced by strong spin-orbit coupling. Our results are valid for weak correlations with large number of bosons. Strongly correlated states, analogous to the fractional quantum Hall states, would emerge with small number of bosons [17]. These can be addressed using exact diagonalization method in future studies.

Acknowledgment — We would like to thank Hui Zhai, Congjun Wu, Xiang-Fa Zhou and Shih-Chuan Gou for useful discussions. HH and XJL were supported by the ARC Discovery Projects (Grant Nos. DP0984522 and DP0984637) and NFRP-China (Grant No. 2011CB921502). HP was supported by the NSF, the Welch Foundation (Grant No. C-1669) and the DARPA OLE program.

Note added. - When our manuscript was under review, we became aware of a preprint [18], in which the authors addressed the same problem at $g = g_{\uparrow\downarrow}$.

[1] X. L. Qi and S. C. Zhang, Physics Today **63**, 33 (2010).
[2] Y.-J. Lin, K. Jiménez-García, and I. B. Spielman, Nature (London) **471**, 83 (2011).
[3] T. D. Stanescu, B. Anderson, and V. Galitski, Phys. Rev. A **78**, 023616 (2008).
[4] C. Wu, I. Mondragon-Shem, and X.-F. Zhou, Chin. Phys. Lett. **28**, 097102 (2011).
[5] J. Larson and E. Sjöqvist, Phys. Rev. A **79**, 043627 (2009).
[6] C. Wang *et al.*, Phys. Rev. Lett. **105**, 160403 (2010).
[7] T.-L. Ho and S. Zhang, Phys. Rev. Lett. **107**, 150403

(2011).
[8] Y. Zhang, L. Mao, and C. Zhang, eprint arXiv:1102.4045.
[9] Z. F. Xu, R. Lü and L. You, Phys. Rev. A **83**, 053602 (2011); T. Kawakami, T. Mizushima, and K. Machida, Phys. Rev. A **84**, 011607(R) (2011).
[10] Y.-J. Lin *et al.*, Nature (London) **462**, 628 (2009).
[11] D. A. Butts and D. S. Rokhsar, Nature (London) **397**, 327 (1999).
[12] X.-J. Liu *et al.*, Phys. Rev. Lett. **87**, 030404 (2001).
[13] A.-C. Ji *et al.*, Phys. Rev. Lett. **101**, 010402 (2008); S.-W. Su *et al.*, Phys. Rev. A **84**, 023601 (2011).
[14] B. Ramachandhran *et al.*, to be published.
[15] T. Yefsah *et al.*, Phys. Rev. Lett. **107**, 130401 (2011).
[16] A. E. Leanhardt *et al.*, Science **301**, 1513 (2003).
[17] N. K. Wilkin and J. M. F. Gunn, Phys. Rev. Lett. **84**, 6 (2000).
[18] S. Sinha, R. Nath, and L. Santos, eprint arXiv:1109.2045.